Wave Force on a Curtain-Wall-Type Breakwater

Due to Obliquely Incident Waves

by

Tsunehiro Sekimoto*, Kosuke Kondo**, Tetsunori Ohshimo*

ABSTRACT
     Assessment of the characteristics of the wave force on
the curtain-wall-type breakwater, due to obliquely incident
waves, was conducted through numerical calculation, labora-
tory and field experiments.   In the numerical calculations,
the Boundary Integral Equation Method (BIEM) for obliquely
incident waves was used.   From the results of calculation
and laboratory experiment, design graphs for estimating
design wave force were established and the validity of the
diagrams was verified through comparison with the results of
laboratory and field experiments.

1. INTRODUCTION
     The curtain-wall-type breakwater is a structure which
has a vertical or inclined rigid thin barrier extending from
above the water surface to some distance below.   An example
of the curtain-wall-type breakwater is shown in Fig. 1.   The
curtain-wall is supported by a jacket which is attached to
the front side steel pile.

     A curtain-wall-type breakwater is often selected as an
inlet structure in the harbors of thermal or nuclear power
plants in Japan, because they need to take in a great amount
of water.   The breakwater is also used as a simple wave
eliminator in order to provide safe anchorage for vessels in
large harbors or fishing ports.   In these cases, the inci-
dent wave direction to the breakwater is usually restricted
since breakwaters are constructed within the harbor.   It is
very important to know the characteristics of the wave force
on the breakwater in relation to the direction of incident
waves.   However, little is known about the characteristics
of the wave force.

     In this study, two types of laboratory experiments and
two series of field experiments were conducted and the
numerical calculation based on Boundary Integral Equation
Method was performed. Based on these experiments and calcu-
lation, the characteristics of wave force on the curtain-
wall-type breakwater due to obliquely incident waves were
discussed, and design graphs for estimating design wave
force for a wide range of incident wave directions were
established.

* Engineer, Design and Engineering Department, Penta-Ocean
   Construction Co., Ltd., 2-2-8 Koraku Bunkyo-ku Tokyo 112
   Japan.
** Principal Engineer, Design and Engineering Department,
   Penta-Ocean Construction Co., Ltd.
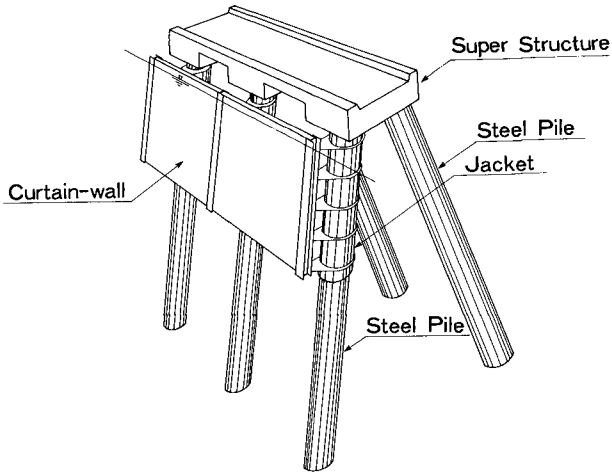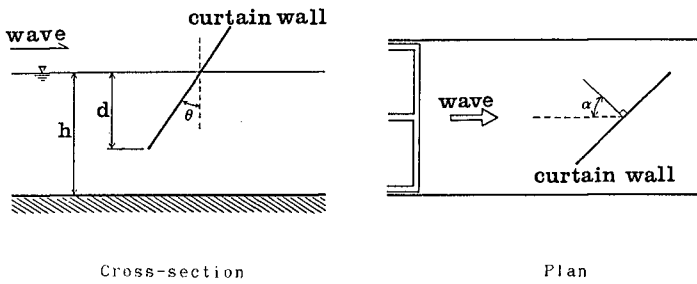
Fig. 1   A curtain-wall-type breakwater

Cross-section   Plan

Fig. 2   Definition sketch of a curtain-wall-type breakwater
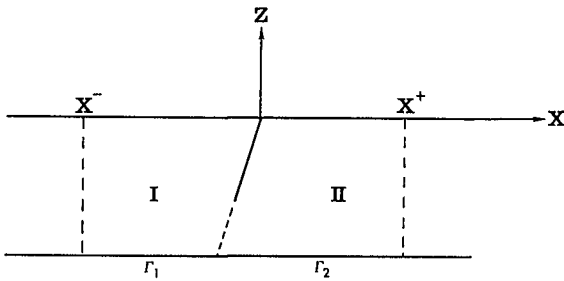

Fig. 3   Computational domain

2.   NUMERICAL CALCULATIONS
     Numerical calculations, which are based on the Boundary
Integral   Equation   Method   (BIEM)   proposed   by   Liu   and
Abbaspour   (1982),   are extended to the cases   of   obliquely
incident   waves   on   the assumption that the length   of   the
breakwater is infinitely long and its shape does not   change
along the breakwater.

     A   definition   sketch of the curtain-wall is   shown   in
Fig. 2.   In   these figures,   α means   incident angle,   θ is
curtain-wall inclined angle, d is the submerged curtain-wall
depth and h means the water depth.

     The sketch of the computational domain is shown in Fig.
3.   Two   auxiliary boundaries X$^+$ and X$^-$ are   introduced   to
utilize   the BIEM technique.   The procedure proposed by Liu
and Abbaspour is characterized by two main points.   One   is
the introduction of a velocity singularity at the tip of the
breakwater,   to aid accurate calculation.   The second is the
division   of   the   calculation region into   two   subregions,
Region I and Region II as shown Fig. 3,   for   simplification
in the treatment of the thin barrier.   The procedure of Liu
and Abbaspour is as follows.

     The   boundary   integral   equation   of   the   Laplace's
Equation is

$$\frac{Cj}{2\pi}f(xj,zj) = \int_{\Gamma j}[f^*\frac{\partial f}{\partial n} - f\frac{\partial f^*}{\partial n}]ds; \quad j=1,2 \tag{1}$$

     Γj is the Boundary in each region.   Cj is the interior
angle at the base point (xj, zj),   ∂/∂n is   the normal diffe-
rential taken positive outwards, r is the distance between a
base   point   to another point on   the   boundary.   When   the
incident   wave direction is normal to the Breakwater,   f   is
the   spatial   variation of the velocity potential and   f   is
defined by

$$\phi(x,y;t) = f(x,z)\exp[-i\sigma t] \tag{2}$$

Where φ is the velocity potential, σ is the angular frequen-
cy,   x,   z is the horizontal and vertical coordinates respec-
tively   and   t   is the time.   The Green's function   of   the
Laplace's Equation f* is

$$f^* = \frac{1}{2\pi}\ln\frac{1}{r} \tag{3}$$

     By discretizing and integrating equation (1) numerical-
ly   and introducing the boundary conditions,   the   solutions
can be obtained.
     The boundary conditions are as follows
     The condition on the surface;

$$\frac{\partial f}{\partial n} = \frac{\sigma^2}{g}f \tag{4}$$

The condition along the bottom and surface of the structure;

$$\frac{\partial f}{\partial n} = 0 \tag{5}$$

The condition along the auxiliary boundaries;

$$f = f^{\pm} \tag{6}$$

$$\frac{\partial f}{\partial n} = \frac{\partial f^{\pm}}{\partial n} \tag{7}$$

f^+ and f^- are presented by

$$f^+ = A_0^+ \frac{\cosh k(z+h)}{\cosh kh} \exp[ikx^+]$$

$$+ \sum_{n=1}^{\infty} A_n^+ \frac{\cos Kn(z+h)}{\cos Knh} \exp[-Knx^+] \tag{8}$$

$$f^- = A_0^- \frac{\cosh k(z+h)}{\cosh kh} \exp[-ikx^-]$$

$$+ \sum_{n=1}^{\infty} A_n^- \frac{\cos Kn(z+h)}{\cos Knh} \exp[Knx^-] + f_I \tag{9}$$

Where K_n is the nth imaginary root of the dispersion relationship, f_I is the velocity potential of the incident wave, $A_0^{\pm}$ are the amplitude of the transmission and the reflection wave and $A_n^{\pm}$ are the amplitude of the scattering waves.

Using a previous assumption, that the length of the breakwater is infinitely long and its shape does not change along the breakwater, the three dimensional Laplace's equation can be reduced to the two dimensional Helmholtz's equation. The boundary integral equation of Helmholtz's equation is also represented by equation (1). Assuming the y axis corresponds to the direction along the breakwater, f is defined by

$$\Phi(x,y,z;t) = f(x,z)\exp[i(ky\sin\alpha - \sigma t)] \tag{10}$$

The Green's function of Helmholtz's equation is described by the modified Bessel's function.

$$f^* = \frac{1}{2\pi}K_0(kr\sin\alpha) \tag{11}$$

Introducing the boundary conditions previously used and using the equations (12) and (13) instead of equations (8) and (9), the solutions can be obtained in the case of obliquely incident waves.

$$f^+ = A_0^+ \frac{\cosh k(z+h)}{\cosh kh} \exp[ikx^+\cos\alpha] \qquad (12)$$

$$f^- = A_0^- \frac{\cosh k(z+h)}{\cosh kh} \exp[-ikx^-\cos\alpha] + f_I \qquad (13)$$

The wave force and the water surface elevations were calculated from the potential f.

3.　LABORATORY AND FIELD EXPERIMENTS

　　One of the experiments is a fundamental study with the curtain-wall in an uniform water depth. A wave-tank which has 34m length, 5m width and 1.2m depth was used. The incident and reflected waves, the transmission waves, the water surface elevation just in front of and just behind the curtain-wall and the wave pressure acting on the breakwater are measured using capacitance type wave gages and small size pressure gages. The models of the breakwater were made from a model unit which consists of steel frame and plywood curtain-wall. In order to reduce the effect of reflected waves from the side-wall and wave-paddle, the partition wall and the wave absorber were arranged for various conditions of incident wave angle. The experimental conditions are shown in Table 1. In the regular wave experiments, four kinds of wave period were used with three kinds of wave height. In the irregular wave experiments, three kinds of significant wave period were used with significant wave height of 8 cm only. Incident wave angle varied in six different directions from 0 to 90 degrees. Three kinds of inclined curtain-wall angle and two types of relative submerged depth d/h were tested. The water depth was set at 60cm in all cases. We carried out more than 200 runs using both regular and irregular waves.

Table-1　The experimental condition

	Regular wave	Irregular wave
Wave Period T, T1/3 (sec)	1.0, 1.5, 2.0, 2.5	1.0, 1.5, 2.0
Wave Height H, H1/3 (cm)	5.0, 8.0, 10.0	8.0
Incident wave angle α (deg)	0, 30, 45, 60, 75, 90	
Inclined angle θ (deg)	0, 20, 45	
Relative submerged depth d/h	0.4, 0.6	

The field experiments were carried out from January through March of 1985, and January through February of 1986, at the port of Kashiwazaki-Kariwa nuclear power plant, Niigata, Japan. Kashiwazaki-Kariwa is located on the Sea of Japan in central Niigata Prefecture and is shown in fig. 4.
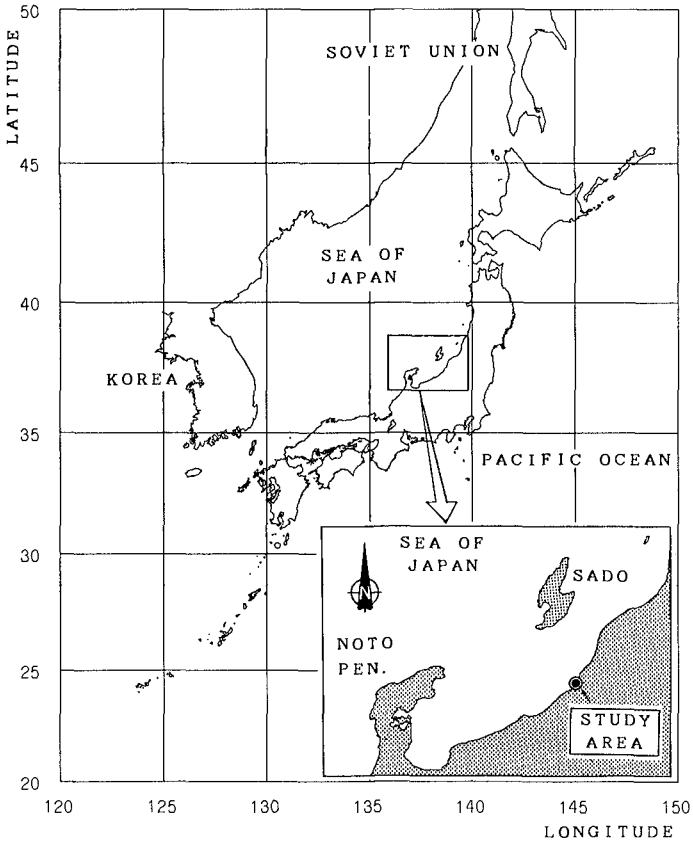
Fig. 4   The location of the investigation site

Fig. 5 is the shape of the port. The north breakwater and the north jetty are on the right hand side and the south breakwater and south jetty are on the left hand side of this figure. The curtain-wall-type breakwater is located in the middle of the south breakwater. The inclined angle and relative submerged depth of this curtain-wall are 15 degrees and 0.6 respectively. The water depth below the curtain-wall is 13 m. The water surface elevations just in front of and just behind the breakwater and the wave pressure on the breakwater are measured in the center section of this curtain-wall-type breakwater. The measurement of the water surface elevations and the wave pressures are performed using two capacitance type wave gages and eight pressure gages respectively.

Another experiment is an 1/80 scale model test of the port of Kashiwazaki-Kariwa nuclear power plant, in a 40 m length and 30 m width wave-tank. Both the water surface elevation and wave force were measured. In this experiment, unidirectional irregular waves, which have the Bretschneider-Mitsuyasu type power spectra, and JONSWAP Spectra, that approximate the field observed power spectra, were used. The water surface elevations were measured using capacitance type wave gages and the wave force measurement were performed by measuring the strain in the steel arm which supports the measuring part, when cut off from the other part of the curtain-wall.

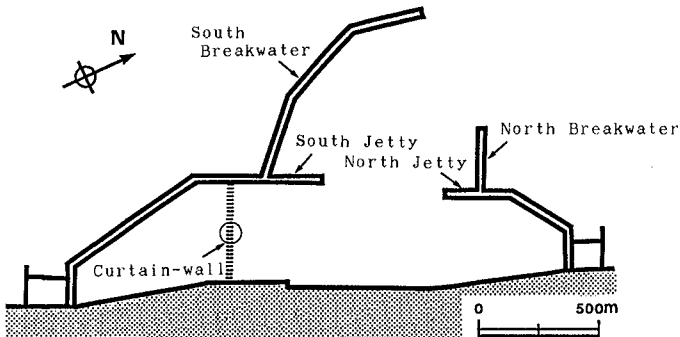The result of the calculations and the laboratory and field experiments were compared.

Fig. 5   Kashiwazaki-Kariwa port

4. COMPARISON BETWEEN RESULTS OF EXPERIMENT AND CALCULATION

Fig. 6 is the comparison of numerical predictions by BIEM with experimental results using regular waves for wave force coefficient as a function of the incident wave angle, with the condition that h/L = 0.201, θ = 20 degrees and d/h = 0.6. The wave force coefficient is defined as the ratio between the wave force per unit curtain-wall length and the incident wave height. The experimental results agree with calculation results with the exception of the large value of α. One of the reasons for this anomaly is that the incident wave energy is transformed into a wave running along the curtain-wall.
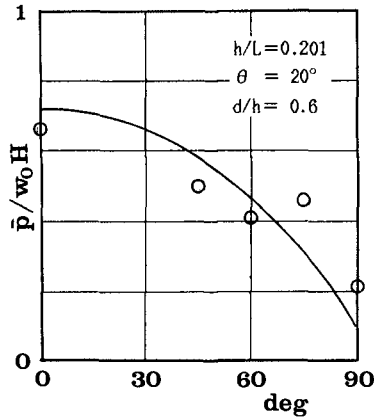
Fig. 6   The comparison between numerical and experimental results for wave force coefficient (regular wave)

The comparison results of irregular waves are shown in Fig. 7. The spectrum analysis is used for analysis of irregular waves. The wave force coefficient is defined as the transfer function of two times surface elevation of the incident wave to the wave force. The relative water depth is calculated from the wave length of each component wave. In the figures, a circle is the result using a wave with 1.5 sec significant wave period and a triangle means a wave of 2.0 sec. These are the results of plotting the wave force coefficient against the relative water depth in the case where θ = 20 degrees and d/h = 0.6.

We obtain relatively good agreement between both, except for the lower range of h/L in the case where α = 30 degrees. In this experiment, for the small incident wave direction, the distance between the edge of the model and the measuring point was short. Thus the effect of the scattering wave from the edge appeared in the result for the case where α = 30 degrees.

For the case of inclined angle θ = 45 degrees, agreement between results was not good because of the effect of the wave runup.

Fig. 8 are the figures showing the ratio of the wave force to the difference of the water level, on both sides of the curtain-wall, against h/L when α = 45 degrees. The results from BIEM fit very well with the experiment results except for the case where θ = 45 degrees. This is due to the effect of the wave runup. It is considered that the effective difference of the water levels is smaller than the measured difference. The ratio for different values of α lies almost on the same line. This fact was also confirmed in model tests and field experiments. Fig. 9 is the example of the result of an 1/80 model test and Fig. 10 is the result of field experiments. Good agreement between the calculation results and the experimental results is found in these figures. This implies that the wave force can be estimated accurately by BIEM if the difference of the water levels on both sides is given. And this fact also means the relations between the wave force and the difference of the water levels on both sides of the curtain-wall are hardly affected by the incident wave angle.

The difference of the water surface elevation on both sides can be separated into the amplitudes of the water surface elevation on both sides and the phase difference of both. Thus investigation followed on the phase difference and the ratio of the amplitude of the water surface elevation just behind the curtain-wall to the one just in front of it.

Fig. 11 shows the results of calculations and experiments on the phase difference between water levels as functions of h/L. It is found that the phase difference decreases as the incident angle of the waves increases. This is due to the increase in the apparent wave length. Agreement of the results of both calculation and experiment is good.

Fig. 12 shows the ratio of the water surface elevation just in front of to just behind the curtain-wall. When α = 30 degrees, the experimental results agree well with the calculation results. However, as the incident wave angle increases, experiment results do not increase although the calculation result increases. This may be due to the fact that a part of the incident wave transformed into the wave running along the curtain-wall, although this is difficult to estimate quantitatively. However, it is found that the amplitude of the water surface elevation just in front of the curtain-wall decreases as the incident wave angle increases, and that the water surface elevation just in front of the curtain-wall and the ratio of the amplitudes of the both sides of the curtain-wall cancel the difference between calculation and experiment.
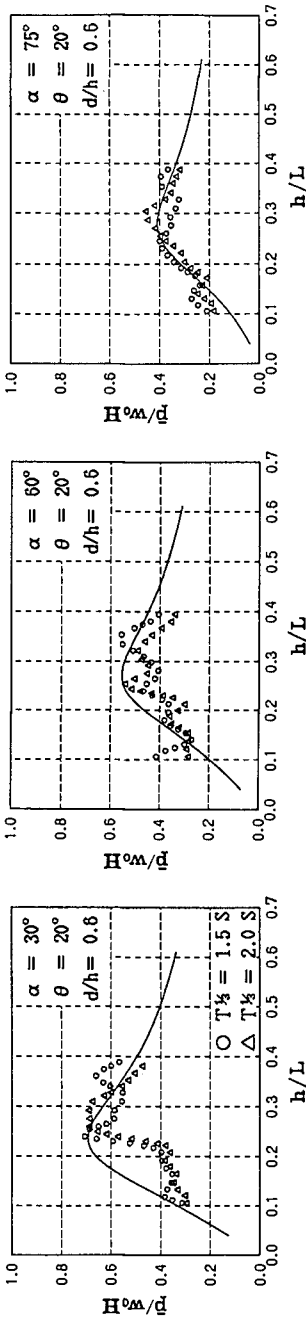
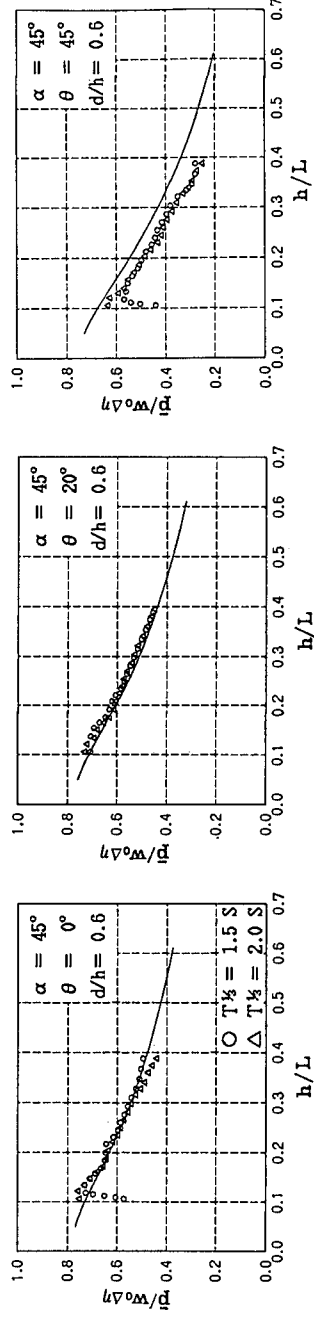Fig. 7   The relation between wave force and incident wave height

Fig. 8   The relation between wave force and the difference in water surface elevations
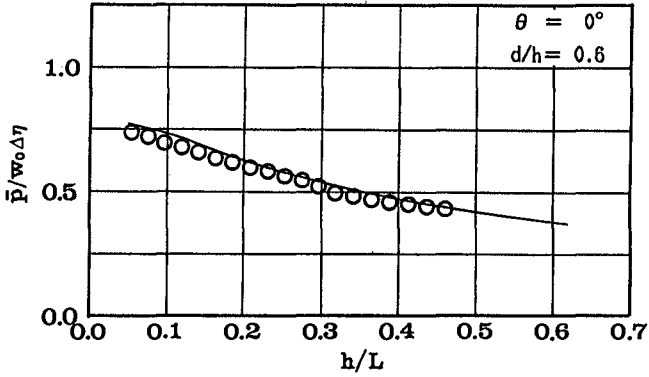
Fig. 9   The relation between wave force and the difference
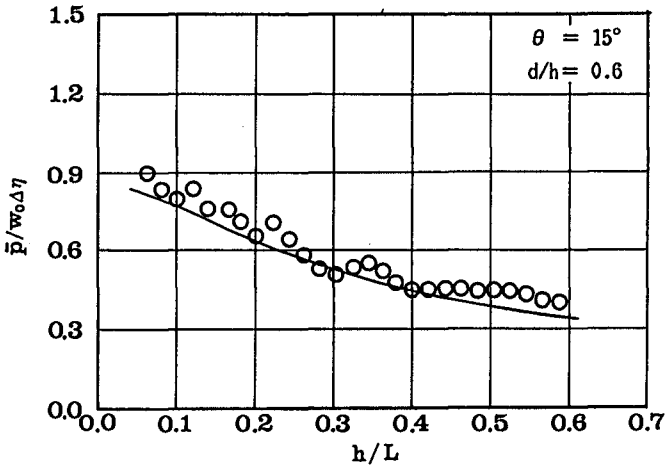   in water surface elevations (1/80 model test)

Fig. 10   The relation between wave force and the difference
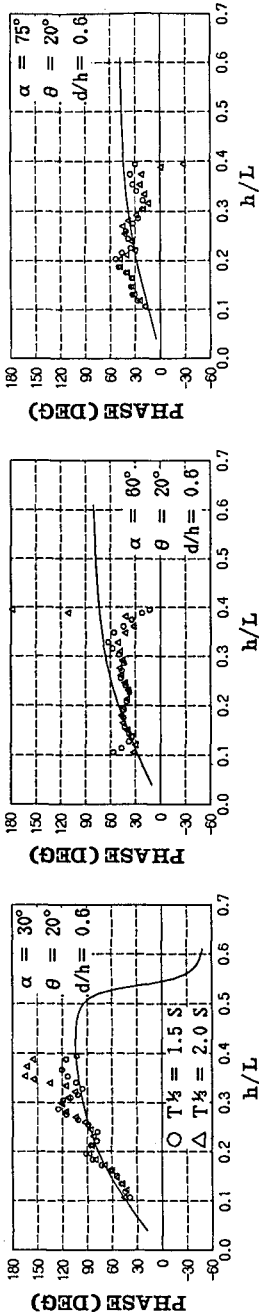   in water surface elevations (field experiment)

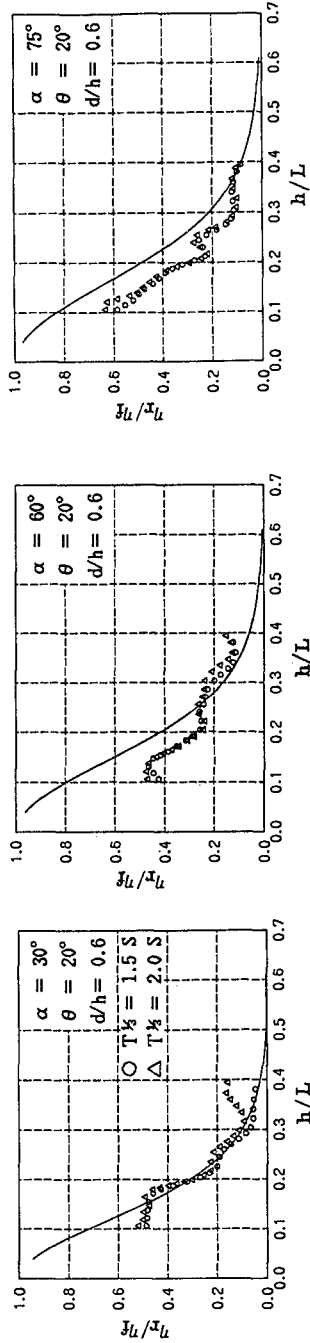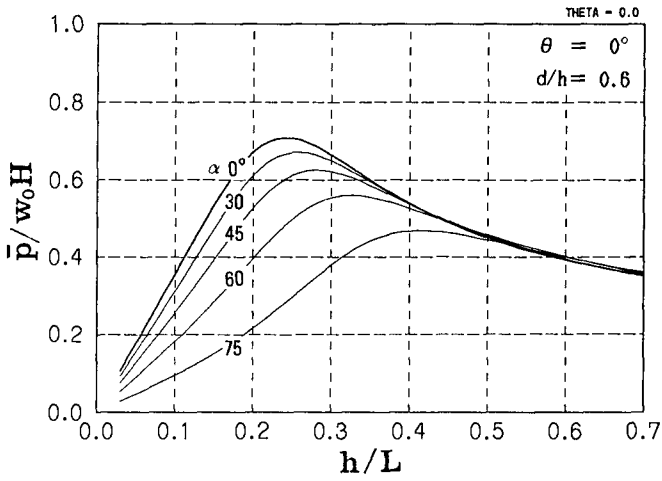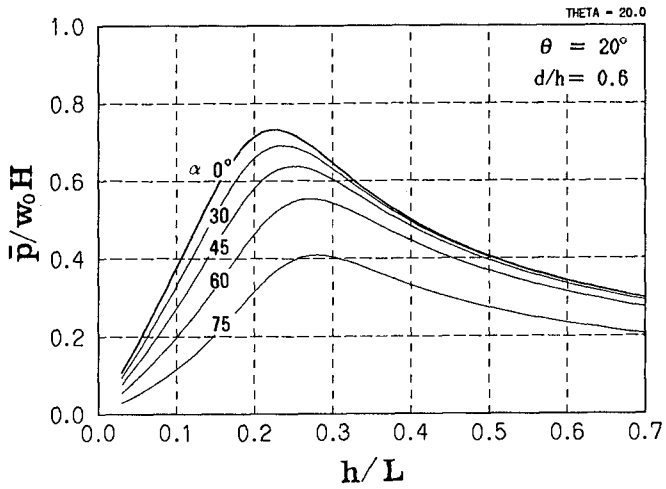Fig. 11 The phase difference between the water surface elevations

Fig. 12 The ratio between the amplitudes of water surface elevations

(a) θ = 0 degree

(b) θ = 20 degrees

Fig. 13   The diagram for estimation of design wave force

5. DESIGN WAVE FORCE

The wave force coefficient for irregular waves can be regarded as a transfer function. In the case of using the representative wave height as the design wave height, the moving weighted average of calculation results using BIEM, where 'weight' is a wave power spectra, is required. However, in consideration of the uncertainty about the mechanism of wave force and the accuracy of the calculation, BIEM results alone can be employed for estimation of design wave force. The diagrams for estimation of design wave force are shown in Fig. 13.

The comparison of numerical predictions with the experimental results of an 1/80 model test on wave force is shown in Fig. 14. In numerical predictions, Green's function method was used for calculation of directional spectra in a harbor {Kondo et al (1987)}. This is an extension of the procedure proposed by Gaillard (1984) in order to estimate the wave height and the wave direction at the measured point of the wave force. We obtained relatively good agreement between the calculation and the experimental results, even although the incident wave angle varied from 45 to 70 degrees.
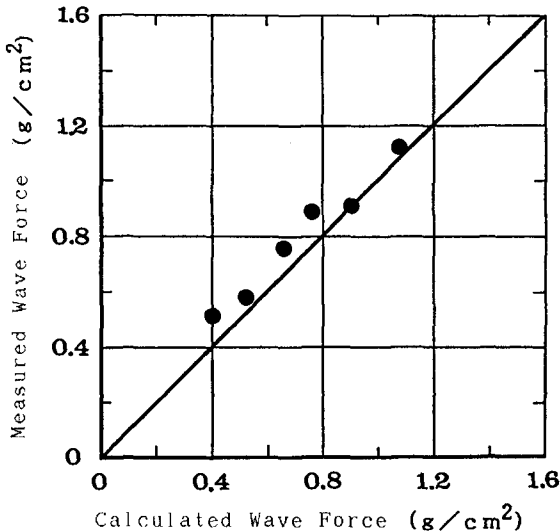
Fig. 14   The comparison of numerical predictions with the experimental results of an 1/80 model test on wave force

6. CONCLUSIONS
    The characteristics of the wave force on the curtain-wall-type breakwater may be determined from the results of calculations based on BIEM and experiments.   As a result, diagrams for estimating design wave force accurately for a wide range of incident wave direction were established. The applicability of this method are confirmed from the results of the 1/80 model test and field investigations.

REFERENCES
[1] GAILLARD, P., Combined refraction-diffraction calcula-
     tions with directional spectra, Proc. 19th Coastal
     Engineering., ASCE , pp.1040-1056, 1984.
[2] KONDO, K., SHIMIZU, T. and YAMADA, K., Green function
     method for calculation of directional wave spectrum in
     a harbor, Proc. 34th Japanese Conf. on Coastal Eng.,
     pp.106-110, 1987 (in Japanese).
[3] LIU, P.L. and ABBASPOUR, M., A wave scattering by a
     rigid thin barrier, J. Wtrway., Port, Coast and Ocean
     Engrg., ASCE, 108, PP.479-491, 1982.